View Article Online
View Journal

ChemComm

Chemical Communications

Accepted Manuscript

This article can be cited before page numbers have been issued, to do this please use: G. Lv, A. Sun, M. Wang, P. Wei, R. Li and T. Yi, *Chem. Commun.*, 2020, DOI: 10.1039/C9CC09233A.

ROYAL SOCIETY OF CHEMISTRY

rsc.li/chemcomm

ROYAL SOCIETY OF CHEMISTRY
View Article Online
DOI: 10.1039/C9CC09233A

Journal Name

COMMUNICATION

A Novel Near-Infrared Fluorescent Probe for Detection of Early-stage Aβ Protofibrils in Alzheimer's Disease

Received 00th January 20xx,
Accepted 00th January 20xx

DOI: 10.1039/x0xx00000x

www.rsc.org/

Guanglei Lv,[a,c] Anyang Sun,*[b] Minqi Wang,[b] Peng Wei,[a] Ruohan Li,[a] and Tao Yi*[a]

Detection of Aβ protofibrils at the early stage of Alzheimer's disease was realized by a novel near-infrared probe (DCM-AN) based on dicyanomethylene-4H-pyran. This probe exhibits high affinity towards Aβ protofibrils *in vitro* and in brain sections of transgenic mouse models for Alzheimer's disease.

Alzheimer's disease (AD) is one of the most prevalent form of neurodegenerative diseases. Unfortunately, so far, there are no effective drugs to cure this disease when clear clinical symptoms appear. In fact, neurodegeneration is estimated to start 10–30 years before clinical symptoms are detected in AD.[1] Therefore, seeking effective probes to monitor the progression of AD is extremely urgent. It is well established that AD has two main pathological hallmarks: β-amyloid plaques composed of β-amyloid peptide (Aβ) and neurofibrillary tangles resulting from hyperphosphorylated Tau protein.[2-6] Biochemical and pathological analyses of AD brain samples reveal that Aβ species exist in several forms, [7] including soluble monomers,[8] oligomers,[9] protofibrils[10,11] and insoluble aggregates.[2]

Initially, much effort had been made on the detection and imaging of Aβ aggregates.[12-16] However, there is increasing evidence that Aβ aggregates burden correlated poorly with the severity of AD,[17, 18] whereas non-monomeric soluble Aβ species exhibit much more toxic than insoluble Aβ aggregates.[19, 20] Among soluble Aβ species, Aβ protofibrils were significantly important intermediate, which were first observed and characterized about two decades ago with rich β-sheet structure as precursors to mature fibrils.[21,22] After that, studies on Aβ protofibrils have attracted extensive interest and an increasing amount of data for the detailed structure of Aβ protofibrils has become available.[23, 24] Previous studies revealed that Aβ protofibrils possess neurotoxicity[25] and neuroinflammation[26] and can disrupt ion channels in rat cortical neurons.[27] These findings demonstrate that Aβ protofibrils play an important role in the progress of AD, especially the early stage of the disease. Therefore, it is greatly urgent to develop effective probes for specifically detecting Aβ protofibrils. However, to the best of our knowledge, no probe capable of specifically targeting and imaging Aβ protofibrils has been reported till now.

Recently, we developed a series of fluorescent probes for specific detection of Aβ aggregates[28] and Aβ oligomers[29] based on aminonaphthalene (AN). Even though it is still a great chellange to distinguish soluble and insoluble Aβ species due to their similar structures, previous works from us and other researchers intented that the appropriate steric hindrance of the fluorophore might be the key point to differentiate those different Aβ species.[30, 31] This is due to the fact that different level of hydrophobic cavities can be produced in the different state of the Aβ assembly.[32, 33] Therefore, design a fluorescent probe with suitable steric hindrance specifically binding with the cavity of Aβ protofibrils is the strategy of this work.

Dicyanomethylene-4H-pyran (DCM) derivatives have attracted significant attention because of their controllable emission wavelength in NIR or far-red area. In addition, DCM derivatives possess large Stokes shift and high photostability. These make DCM derivatives better candidates for fluorescence imaging.[34-35] Since DCM has certain steric hindrance, we envision that, by modifying the structure of DCM moiety, it might be possible to develop a novel probe capable of detecting Aβ protofibrils with good affinity and specificity. Therefore, the fluorescent probe **DCM-AN**, combining DCM moiety with Aβ target group AN (Scheme 1), was designed and synthesized to investigate its specificity toward Aβ protofibrils. To our delight, **DCM-AN** is capable of detecting Aβ protofibrils from Aβ species and can image Aβ protofibrils in the brain of transgenic mouse models.

[a.] *Department of Chemistry, Fudan University, Shanghai 200438, P. R. China. E-mail: yitao@fudan.edu.cn.*
[b.] *Laboratory of Neurodegenerative Diseases and Molecular Imaging, Shanghai University of Medicine & Health Sciences, Shanghai 201318, P. R. China E-mail: sunay@sumhs.edu.cn*
[c.] *Key Laboratory of the Ministry of Education for Advanced Catalysis Materials, Zhejiang Normal University, Jinhua 321004, P. R. China*
† Footnotes relating to the title and/or authors should appear here.
Electronic Supplementary Information (ESI) available: [synthetic details and additional spectra and images]. See DOI: 10.1039/x0xx00000x

View Article Online
DOI: 10.1039/C9CC08373A

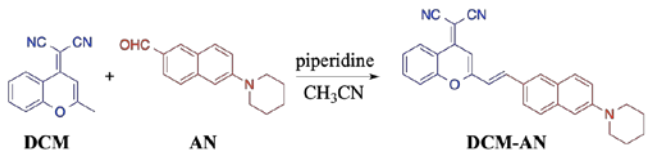

Scheme 1. Structure and synthesis route of **DCM-AN**

Fluorescence spectroscopy experiments were performed to investigate the binding properties of **DCM-AN** with Aβ. **DCM-AN** has a typical D-π-A structure with dicyanomethylene as an electron accepter and piperidine as an electron donor. The rotation of the ethylene group makes the molecule poor internal charge transfer (ICT) process and low fluorescence in water and polar solvent. Therefore, the fluorescence of **DCM-AN** was very weak in the phosphate buffered saline (PBS) solution (Fig. 1). The maximum fluorescence emission peak lying in 725 nm with absolute fluorescence quantum yield (Φ_F) of 0.06%. However, when Aβ protofibrils (determined by dynamic light scattering and TEM (Fig. S2) were added to the PBS solution of **DCM-AN**, the fluorescence intensity was significantly increased (Fig. 1A). The emission peak was blue shifted from 725 to 661 nm, while Φ_F value increased to 1.5%. This indicated that **DCM-AN** showed high binding activity with Aβ protofibrils. By contrast, the fluorescence intensity of **DCM-AN** showed little change in the presence of Aβ aggregates or monomers (Fig. 1A). Furthermore, even though the concentration of Aβ peptides in aggregates was four times as that in protofibrils, the fluorescence intensity of **DCM-AN** was still very weak for Aβ aggregates (Fig. S3). While the fluorescence intensity of **DCM-AN** gradually increased to some extent in the presence of Aβ oligomer since the structure of oligomers is more closely related to protofibrils,[36] but the intensity was lower than that of Aβ protofibrils. These suggest that **DCM-AN** exhibits good specificity towards Aβ protofibrils. It could be seen from Fig. 1B that the fluorescence intensity of **DCN-AN** did not show remarkable enhancement with another aggregated peptide amylin (an aggregation-prone 37-residue peptide secreted together with insulin by pancreatic B cells). Furthermore, little fluorescence changes were observed when human serum albumin (HSA) or tau protein was added (Fig. S4).

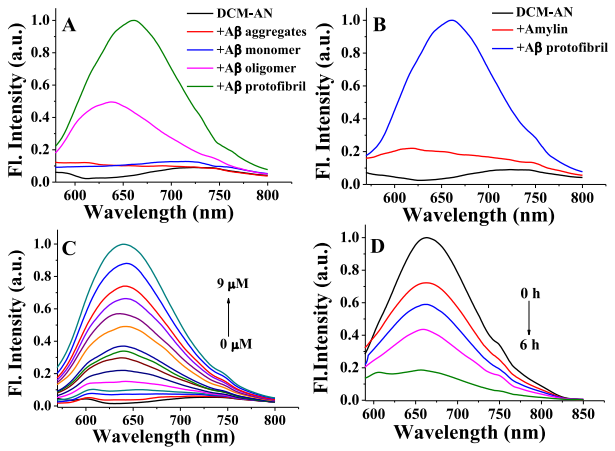

Fig. 1. Fluorescence spectra of **DCM-AN** (2.0 μM) with (A) Aβ species (5.0 μM), (B) another peptide Amylin (5.0 μM), (C) different Aβ protofibril concentrations (0-9 μM) and (D) different incubation time of Aβ protofibrils (5.0 μM),), λ_{ex}=500 nm.

In addition, DCM-AN showed high anti-interference ability toward common cations and anions (Fig. S5). Subsequently, titration experiment was performed under different concentrations of Aβ protofibrils (0-9 μM, Fig. 1C). Linear relationship was observed between the concentration of Aβ protofibrils and the fluorescence intensity of **DCM-AN** (R^2 = 0.98, Fig. S6). Furthermore, the dissociation constant of **DCM-AN** for Aβ protofibrils was measured to be 0.85 μM (Fig. S1).

Since **DCM-AN** showed high affinity towards Aβ protofibrils, the dynamic aggregation process of Aβ protofibrils was then traced by the change of fluorescence intensity of **DCM-AN** with different incubation time (Fig. 1D). It could be easily found that there was an enhanced fluorescence intensity in the PBS solution after the addition of Aβ protofibrils. As expected, the fluorescence intensity of **DCM-AN** decreased upon prolonging the incubation time because Aβ protofibrils grew to mature fibrils. This data further confirmed that **DCM-AN** exhibited high affinity towards Aβ protofibrils. In addition, the detection limit of this probe for Aβ protofibrils was measured to be 51.9 nM (Fig. S7), which is sensitive enough to detect Aβ species in physiological concentration.

To study the binding mechanism of **DCM-AN** with Aβ protofibrils, quantum mechanical calculations were performed for **DCM-AN** followed by a molecular docking search and molecular dynamics simulations for the complex of **DCM-AN** and Aβ protofibrils. Firstly, the optimized structure of **DCM-AN** (Fig. 2A) was obtained in the gas phase based on quantum mechanical calculations at the B3LYP/6-31G level using Gaussian 09 software package. Secondly, molecular docking search between **DCM-AN** and Aβ protofibrils model was carried out. Generally, the aggregation degree of protofibrils is more serious than that of oligomers. Therefore, we adopted two different Aβ aggregation intermediates, trimer and dodecamer, as working models for Aβ oligomer and protofibrils, respectively (Fig. S8, A and B). In addition, two different types of Aβ aggregation were chosen as Aβ aggregates working models (Fig. S8 C: PDB ID: 5KK3 and D: PDB ID: 2LMP), which are structurally more complicated than Aβ protofibrils. Through molecular docking search, the binding energy of **DCM-AN** with dodecamer (-12.91 kcal/mol) is lower than that with trimer (-9.15 kcal/mol) and aggregates (Fig. 2C: -10.65 kcal/mol, Fig. 2D: -10.78 kcal/mol). This suggests that **DCM-AN** binds more tightly with dodecamer than with trimer or aggregates. Subsequently, molecular dynamics (MD) simulations were carried out between **DCM-AN** and these Aβ working models (Fig. S8 and S9). As expected, the result of molecular dynamics research exhibits high conformity with the molecular docking.

In addition, the solvent accessible surface area (SASA) was calculated before and after binding between **DCM-AN** and Aβ protofibrils to further illustrate the binding specificity. SASA is the surface area of a biomolecules that is accessible to a solvent.[37] When the probe **DCM-AN** combined with Aβ, it would result in the shrink of SASA to some extent. The more tightly **DCM-AN** binds with Aβ, the more shrinking of SASA is. It is obvious that all of the SASA shrink after **DCM-AN** binds with four Aβ working models (Fig. S6, Table S1), indicating that **DCM-AN** tends to bind with protein owing to the solvent impact.

View Article Online
DOI: 10.1039/C9CC09237A

However, it is noted that the SASA with dodecamer (ΔSASA = 141.491 Å^2) shrinks much more than that with trimer (ΔSASA = 130.584 Å^2, Table S1) or aggregates (ΔSASA = 6.068 Å^2 and 16.707 Å^2 for 5KK3 and 2LMP, respectively, Table S1), indicating that **DCM-AN** binds stronger with Aβ protofibrils than with small oligomer and Aβ aggregates. It is clear that after binding with Aβ protofibrils, the rotation of both ethylene and piperidine groups are restrained, resulting in more effective ICT process and enhancement of the fluorescence.

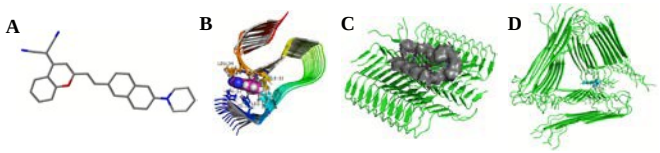

Fig. 2. Calculated binding model of **DCM-AN** with Aβ protofibrils. (A) Optimized structure of **DCM-AN** at B3LYP/6-31G* level; Molecular docking model of **DCM-AN** with Aβ protofibrils (B) and Aβ aggregates (C and D).

Cytotoxicity is an important indicator for a probe applied in bio-research. In order to evaluate the cytotoxicity of **DCM-AN**, MTT assay was performed. The cellular viabilities were estimated to be greater than 90% after 36 hours in the presence of 1-100 μM **DCM-AN** (Fig. S10), indicating that **DCM-AN** showed low cytotoxicity and could further use as a marker of Aβ protofibrils.

Subsequently, we investigate whether this probe **DCM-AN** can specifically target Aβ protofibrils from the brain sections of AD transgenic mouse models. We chose four-month age 5XFAD transgenic mice as AD pathology animal models, because mice have few Aβ mature fibrils (plaques) under four-month age and Aβ mainly exists in form of soluble Aβ species[31, 38-41] while Aβ protofibrils is one of important soluble species.[23] The brain slices of transgenic mouse model stained with **DCM-AN** showed obvious fluorescence signals, whereas the brain slices without **DCM-AN** staining emitted little fluorescence signals (Fig. S11).

To confirm the fluorescence originating from the probe **DCM-AN** combining Aβ protofibrils in the brain section from AD transgenic mouse models under four-month age, colocalization experiments were carried out with Aβ oligomer-specific antibody since Aβ protofibrils are structurally more closely correlated with Aβ oligomers than Aβ aggregates/fibrils,[36] Aβ fibrils specific antibody (OC) and tau antibody. The brain sections were also stained with nucleus staining dye (DAPI) for clarity about the region of experimental brain sections. As expected, **DCM-AN** could co-localized well with Aβ oligomer-specific antibody either in the cerebral cortex or hippocampus (Fig. 3, A-H). However, **DCM-AN** showed poor co-localization with Aβ fibrils OC antibody (Fig. 3, I-L) and tau antibody (Fig. S12).

To further confirm the specificity of **DCM-AN** towards Aβ protofibrils in the brain section, pAβ antibody was chosen to stain Aβ species in the brain sections from AD transgenic mouse models with different ages at early (4, 5-month old), middle (9-month old) and late stage (15-month old) of Aβ pathology for comparison. The images displayed high colocalization between **DCM-AN** and pAβ antibody for four- and five-month age transgenic mice (Fig. 4, A-C and B-F), indicating that **DCM-AN** could efficiently label Aβ pathology at the early stage. With the age increasing (9-month old), the size of Aβ was getting larger compared with 4 and 5-month old mice (Fig. 4H, B and E). However, **DCM-AN** still stained early Aβ species (Fig. 5G, left arrows), while a few plaques were not labeled by **DCM-AN** (Fig. 4G-I, arrowheads). These suggest that **DCM-AN** detects the early Aβ pathology more efficiently at 4- and 5-month old and the favorable efficiency in detecting lasts until 9-month old, even though a little decrease is observed at this age.

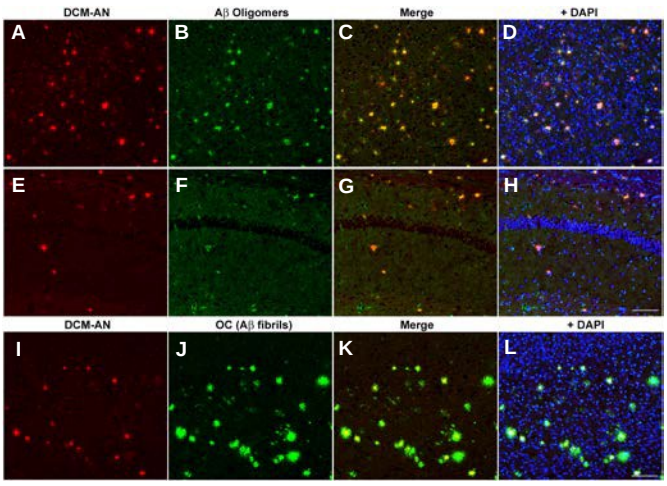

Fig. 3. Colocalization of **DCM-AN** labeling (A, E, I) with immunostaining of Aβ oligomers (B, F) and Aβ fibrils (OC antibody, J) in the brain sections of APP/PS1 transgenic mice. (A)-(D) and (I)-(L) cerebral cortex; (E)-(H) hippocampus. C, G and K are the merge images of DCM-AN and Aβ antibody. DAPI is added in D, H and L. Scale bar: 100 μm.

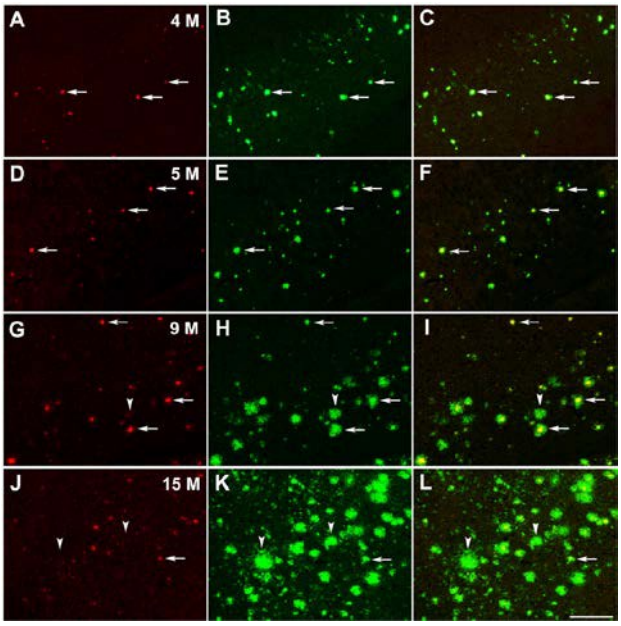

Fig. 4. Detection profile of **DCM-AN** towards Aβ species at different stages of Aβ pathology in the brain sections of APP/PS1 transgenic mice, as compared with Aβ immunostaining; (A-C) and (D-F) early stage of 4-month and 5-month old, respectively; (G-I) middle stage of 9-month old; and (J-L) late stages of 15-month old. A, D, G and J were **DCM-AN** staining; B, E, H and K were Aβ immunostaining with a polyclonal Aβ antibody (pAβ). C, F, I and L were merged images. Left arrows displayed the early stage of Aβ pathology stained by **DCM-AN** and pAβ; arrowheads displayed the late stage of Aβ pathology which could be detected by pAβ but not by **DCM-AN**; scale bar: 200 μm.

For 15-month transgenic mice, mature fibrils/plaques were predominant in the brain sections and Aβ plaques became relatively lager than that of younger transgenic mice. However, small amount of early Aβ species (protofibrils/oligomers) could still be labeled by **DCM-AN** by comparison of the images with pAβ (Fig 4, J-L, marked with left arrows). It was easy to find that mature plaques were not decetced by **DCM-AN** at the late stage of Aβ pathology (Fig. 4, J-L, marked with arrowheads). The result indicated that **DCM-AN** staining exhibited age-dependent and this probe detected tiny or early Aβ pathology in different ages of transgenic mice. By contrast, Aβ immunostaining did not differentiate early and late stages of Aβ pathology. Taken all together, **DCM-AN** detects the early Aβ pathology more efficiently in Alzheimer's transgenic mouse model and displays age dependent in the brain sections.

In order to further confirm that **DCM-AN** may detect Aβ protofibrils, we have performed a comparative staining study with **DCM-AN** and another known red-emitting fluorescent probe, namely QM-FN-SO3, which shows high affinity towards Aβ fibrils.[42] As the data shown (Fig. S13), QM-FN-SO3 presented very weak fluorescence in the brain sections of 4-month-old AD transgenic mice (Fig. S13, A and C), whereas **DCM-AN** clearly stained the early stage of Aβ species that could be Aβ protofibrils (Fig. S13, B and D). In addition, it can be seen that **DCM-AN** shows a very high signal to noise ratio with little intereference of background fluorescence. Taken all together, **DCM-AN** is an excellent probe for dectecting early Aβ pathology.

In conclusion, we designed and synthesized a new fluorescent probe **DCM-AN** capable of detecting Aβ protofibrils. This probe exhibits high affinity towards Aβ protofibrils with a considerably low limit of detection in solution. Moreover, **DCM-AN** shows high affinity towards the early Aβ pathology and is the most likely to bind to Aβ protofibrils/oligomers in brain sections from AD mouse models. Further studies of this probe in the application of in vivo imaging is ongoing in our laboratory.

The authors acknowledge the financial support from NNSFC (21877013, 21671043 and 51872263), Zhejiang Provincial Natural Science Foundation of China (LZ19E020001 and LQ19B050003). We also appreciate the help from Prof. Zhiqian Guo and Prof. Weihong Zhu for providing the compound QM-FN-SO3.

Notes and references

1 E. Giacobini and R. E. Becker, *J. Alzheimer's Dis.*, 2007, **12**, 37.
2 I. W. Hamley, *Chem. Rev.*, 2012, **112**, 5147.
3 K. P. Kepp, *Chem. Rev.*, 2012, **112**, 5193.
4 A. Rauk, *Chem. Soc. Rev.*, 2009, **38**, 2698.
5 K. S. Kosik, *Science*, 1992, **256**, 780.
6 Y. Huang and L. Mucke, *Cell*, 2012, **148**, 1204.
7 K. Rajasekhar, M. Chakrabarti and T. Govindaraju, *Chem. Commun.*, 2015, **51**, 13434.
8 J. T. Jarrett, E. P. Berger and P. T. Lansbury, Jr., *Biochemistry*, 1993, **32**, 4693.
9 P. Verwilst, H. S. Kim, S. Kim, C. Kang and J. S. Kim, *Chem. Soc. Rev.*, 2018, **47**, 2249.
10 J. D. Harper, S. S. Wong, C. M. Lieber and P. T. Lansbury, Jr., *Biochemistry*, 1999, **38**, 8972.
11 A. Abbott, *Nature*, 2008, **456**, 161.
12 L. Cai, R. B. Innis and V. W. Pike, *Curr. Med. Chem.*, 2007, **14**, 19.
13 C. C. Rowe and V. L. Villemagne, *J. Nucl. Med. Technol.*, 2013, **41**, 11.
14 K. Rajasekhar, N. Narayanaswamy, N. A. Murugan, K. Viccaro, H.-G. Lee, K. Shah and T. Govindaraju, *Biosens. Bioelectron.*, 2017, **98**, 54.
15 K. Rajasekhar, N. Narayanaswamy, N. A. Murugan, G. Kuang, H. Agren and T. Govindaraju, *Sci. Rep.*, 2016, **6**, 23668.
16 J. Hatai, L. Motiei and D. Margulies, *J. Am. Chem. Soc.*, 2017, **139**, 2136.
17 X. Zhang, Y. Tian, C. Zhang, X. Tian, A. W. Ross, R. D. Moir, H. Sun, R. E. Tanzi, A. Moore and C. Ran, *Proc. Natl. Acad. Sci. U. S. A.*, 2015, **112**, 9734.
18 C. Ran, X. Xu, S. B. Raymond, B. J. Ferrara, K. Neal, B. J. Bacskai, Z. Medarova and A. Moore, *J. Am. Chem. Soc.*, 2009, **131**, 15257.
19 Y.-M. Kuo, M. R. Emmerling, C. Vigo-Pelfrey, T. C. Kasumic, J. B. Kirkpatrick, G. H. Murdoch, M. J. Ball and A. E. Roher, *J. Biol. Chem.*, 1996, **271**, 4077.
20 L. K. Gouwens, N. J. Makoni, V. A. Rogers and M. R. Nichols, *Brain Research*, 2016, **1648**, 485.
21 J. D. Harper, S. S. Wong, C. M. Lieber and P. T. Lansbury, Jr., *Chem. Biol.*, 1997, **4**, 119.
22 D. M. Walsh, A. Lomakin, G. B. Benedek, M. M. Condron and D. B. Teplow, *J. Biol. Chem.*, 1997, **272**, 22364.
23 H. A. Scheidt, I. Morgado, S. Rothemund, D. Huster and M. Faendrich, *Angew. Chem., Int. Ed.*, 2011, **50**, 2837.
24 N. L. Fawzi, J. Ying, R. Ghirlando, D. A. Torchia and G. M. Clore, *Nature*, 2011, **480**, 268.
25 D. M. Walsh, D. M. Hartley, Y. Kusumoto, Y. Fezoui, M. M. Condron, A. Lomakin, G. B. Benedek, D. J. Selkoe and D. B. Teplow, *J. Biol. Chem.*, 1999, **274**, 25945.
26 G. S. Paranjape, S. E. Terrill, L. K. Gouwens, B. M. Ruck and M. R. Nichols, *J. Neuroimmune Pharmacol*, 2013, **8**, 312.
27 B. O'Nuallain, D. B. Freir, A. J. Nicoll, E. Risse, N. Ferguson, C. E. Herron, J. Collinge and D. M. Walsh, *J. Neurosci.*, 2010, **30**, 14411.
28 G. Lv, B. Cui, H. Lan, Y. Wen, A. Sun and T. Yi, *Chem. Commun.*, 2015, **51**, 125.
29 G. Lv, A. Sun, P. Wei, N. Zhang, H. Lan and T. Yi, *Chem. Commun.*, 2016, **52**, 8865.
30 Y. Li, J. Yang, H. Liu, J. Yang, L. Du, H. Feng, Y. Tian, J. Cao and C. Ran, *Chem. Sci.*, 2017, **8**, 7710.
31 A. G. Kreutzer and J. S. Nowick, *Acc. Chem. Res.*, 2018, **51**, 706.
32 M. Townsend, G. M. Shankar, T. Mehta, D. M. Walsh and D. J. Selkoe, *J. Physiol.*, 2006, **572**, 477.
33 Y. Cheng, B. Zhu, Y. Deng and Z. Zhang, *Anal. Chem.*, 2015, **87**, 4781.
34 Y. Cheng, B. Zhu, X. Li, G. Li, S. Yang and Z. Zhang, *Bioorg. Med. Chem. Lett.*, 2015, **25**, 4472.
35 H. A. Scheidt, I. Morgado and D. Huster, *J. Biol. Chem.*, 2012, **287**, 22822.
36 B. Lee and F. M. Richards, *J. Mol. Biol.*, 1971, **55**, 379.
37 X. Zhang, Y. Tian, Z. Li, X. Tian, H. Sun, H. Liu, A. Moore and C. Ran, *J. Am. Chem. Soc.*, 2013, **135**, 16397.
38 K. Hsiao, P. Chapman, S. Nilsen, C. Eckman, Y. Harigaya, S. Younkin, F. Yang and G. Cole, *Science*, 1996, **274**, 99.
39 D. R. Borchelt, G. Thinakaran, C. B. Eckman, M. K. Lee, F. Davenport, T. Ratovitsky, C.-M. Prada, G. Kim, S. Seekins, D. Yager, H. H. Slunt, R. Wang, M. Seeger, A. I. Levey, S. E. Gandy, N. G. Copeland, N. A. Jenkins, D. L. Price, S. G. Younkin and S. S. Sisodia, *Neuron*, 1996, **17**, 1005.
40 B. Delatour, M. Guegan, A. Volk and M. Dhenain, *Neurobiol Aging*, 2006, **27**, 835.
41 W. Fu, C. Yan, Z. Guo, J. Zhang, H. Zhang, H. Tian and W.-H. Zhu, *J. Am. Chem. Soc.*, 2019, **141**, 3171.

View Article Online
DOI: 10.1039/C9CC09233A

TOC for CC